SMALL-x PHYSICS

A. H. Mueller*
Department of Physics, Columbia University
New York, New York 10027, USA

ABSTRACT

After a brief review of the kinematics of deep inelastic lepton-proton scattering, the parton model is described. Small-x behavior coming from DGLAP evolution and from BFKL evolution is discussed, and the two types of evolution are contrasted and compared. Then a more detailed discussion of BFKL dynamics is given. The phenomenology of small-x physics is discussed with an emphasis on ways in which BFKL dynamics may be discussed and measured.

*This research is supported in part by the Department of Energy under GRANT DE-FG02-94ER40819.

1 Introduction

Small-x physics encompasses those high-energy reactions where there is a hard scattering (at scale Q) and where $s/Q^2 >> 1$ with s the square of the center-of-mass energy of the reaction. Thus, deep inelastic lepton-proton scattering at small values of the Bjorken x-variable is a small-x reaction as is jet production at the Tevatron so long as the transverse momentum of the jet is much less than the center-of-mass energy. The new element which occurs in small-x reactions is that there are two large logarithms present, namely, $\ell nQ^2/\Lambda^2$ and $\ell n1/x$. We are used to summing $(\alpha\ \ell n\ Q^2/\Lambda^2)^n$ corrections as part of ordinary QCD evolution, and this summation is governed by the renormalization group, or equivalently by the Dokshitzer, Gribov, Lipatov, Altarelli, Parisi (DGLAP) [1-3] equation. The resummation of $(\alpha\ \ell n\ 1/x)^n$ terms is less familiar. The leading series of $\alpha\ \ell n\ 1/x$ terms is governed by the Balitsky, Fadin, Kuraev, Lipatov (BFKL) [4-6] equation, and one expects a generalization of the BFKL kernel also to apply to nonleading series of $(\alpha\ \ell n\ 1/x)$ logarithms. The BFKL resummation is more like that which occurs in Regge pole models than that of the renormalization group.

When Q^2 is large and when $\alpha\ell n1/x \geq 1$, in principle one must take into account both resummation in $\ell nQ^2/\Lambda^2$ and in $\ell n1/x$. The DGLAP formalism is sufficiently general to allow this, although resummation of $\ell n1/x$ terms means dealing with anomalous dimensions and coefficient functions to all orders in α. We shall come back to this question in some detail in Sec. 3.

Evolution in Q^2, coming from the DGLAP equation, has been studied and tested in great detail in moderate x reactions. The physics is that of revealing partonic substructure as one probes shorter distance scales, a physics that is well-understood in the framework of perturbative QCD.

Evolution in x, coming from the BFKL equation, has not yet been tested. As one goes to smaller and smaller values of x, at a given short-distance scale, BFKL evolution predicts a growth in hard scattering cross sections due to a growing number of partons. At very small values of x, unitarity corrections are expected to slow the rate of growth of these amplitudes while the growing numbers of overlapping partons (mainly gluons) are expected to initiate a strong field strength regime of QCD where $F_{\mu\nu} \geq 1/g$ and where new nonperturbative QCD effects may appear. The experimental study of BFKL evolution is the most pressing problem in small-x physics, and I shall discuss these issues in some detail in Sec. 6.

These lectures are meant to be an introduction to the theoretical and phenomenological issues in small-x physics with technical details suppressed as much as possible.

2 Structure Functions, the Parton Model, and DGLAP Evolution

2.1 Deep Inelastic Scattering Structure Functions

The cross section for deep inelastic lepton-proton scattering is given, in the proton rest system, by

$$\frac{d\sigma}{dE'd\Omega'} = \frac{4\alpha_{em}^2(E')^2}{Q^4}\left[W_2 cos^2\theta/2 + 2W_1 sin^2\theta/2\right], \tag{1}$$

where the process is illustrated in Fig. 1. E' and Ω' are the energy and scattering solid angle of the outgoing lepton, while θ is the scattering angle between the incoming and outgoing lepton directions. $Q^2 = -q_\mu q_\mu$ is the virtuality of the photon exchanged between the lepton and the proton. The structure functions W_1 and W_2 appear in the decomposition of

$$W_{\mu\nu} = \frac{4\pi^2 E_p}{M}\int d^4x e^{iq\cdot x}(p|j_\mu(x)j_\nu(0)|p) \tag{2}$$

as

$$W_{\mu\nu} = -(g_{\mu\nu} - \frac{q_\mu q_\nu}{q^2})W_1 + \frac{1}{M^2}[p_\mu p_\nu - \frac{p\cdot q}{q^2}(p_\mu q_\nu + p_\nu q_\mu) + (\frac{p\cdot q}{q^2})^2 q_\mu q_\nu]W_2. \tag{3}$$

W_1 and W_2 depend on Q^2 and on the scaling variable $x = \frac{Q^2}{2p\cdot q}$.

2.2 The Bjorken Frame

The parton picture is only manifest in a special infinite momentum (Bjorken) frame where

$$p_\mu = (p_0, p_1, p_2, p_3) \approx (p + \frac{M^2}{2p}, 0, 0, p) \tag{4a}$$

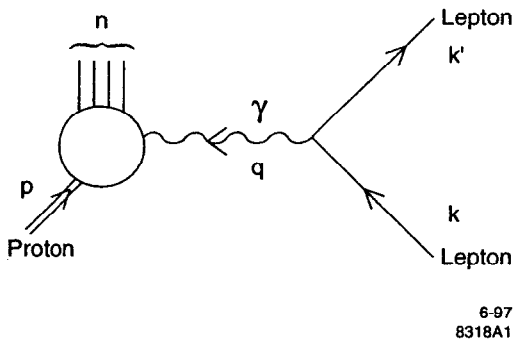

Figure 1.

with p very large and where

$$q_\mu = (q_0, \underline{q}, q_3 = 0). \tag{4b}$$

One can evaluate $q_0 \approx \frac{p\cdot q}{p} \to 0$ as $p \to \infty$ so that

$$Q^2 \approx \underline{q}^2. \tag{5}$$

2.3 The Parton Model (Physical Picture)

In order to describe how the parton model comes about, it is convenient to write

$$W_{\mu\nu} = 2Im\ T_{\mu\nu}, \tag{6}$$

where

$$T_{\mu\nu} = i\frac{4\pi^2 E_p}{M}\int d^4x e^{iq\cdot x}(p|Tj_\mu(x)j_\nu(0)|p) \tag{7}$$

is the time-ordered product of two electromagnetic currents in a proton state. $T_{\mu\nu}$ is given in terms of Feynman diagrams in contrast to $W_{\mu\nu}$ where certain intermediate states are put on mass shell, consistent with $W_{\mu\nu}$ being related to a cross section rather than a scattering amplitude. $T_{\mu\nu}$ is simply the forward Compton amplitude for virtual photon-proton scattering.

Let us follow the time-ordered sequence of a proton absorbing a virtual photon and then reemitting it as given by $T_{\mu\nu}$ in Eq. (7). Since the incoming photon has a transverse momentum Q, it must be absorbed over a transverse spatial size $\Delta x_\perp \sim 1/Q$. We view the proton as a collection of quarks and gluons spread over a transverse size of about one fermi. Because $\Delta x_\perp \sim 1/Q$ is much less than a fermi, the incoming photon will be absorbed by a single quark, the probability of finding two or more quarks in $\Delta x_\perp \sim 1/Q$ being very unlikely. The quark which absorbs the photon is called the struck quark. The lifetime of the struck quark, after absorbing the incoming photon, is

$$\tau \approx \frac{2}{Q}\cdot\frac{k}{Q} = \frac{2k}{Q^2}, \tag{8}$$

with the first factor being the typical virtuality of the struck quark and k/Q, with k the longitudinal momentum of the struck quark, being the time dilation factor. But the "normal" time scale for soft interactions between quarks in a high-momentum parton is $\tau_0 = \frac{2p}{\mu^2}$ with $\mu \approx 300\ MeV$. Thus, the struck quark is in the uncomfortable situation of having a lifetime much too short, and a transverse momentum much too large, to fit into the proton's infinite momentum wavefunction. In order to fit into the wavefunction, the struck quark will reemit the virtual photon, thus lowering its transverse momentum and increasing its lifetime to that of a normal quark in the light-cone wavefunction of a proton. The picture is illustrated in Fig. 2. Thus, in the Bjorken frame, the virtual photon resolves individual quarks and measures them with a resolution $\Delta x_\perp \sim 1/Q$.

2.4 The Parton Model (Formulas)

We have just seen that the virtual Compton amplitude can be viewed as the absorption of the photon by the struck quark followed by the reemission of the photon by the same quark. This suggests that the virtual photon actually determines, or measures, the single-quark distribution in the proton. This is stated quantitatively by the formula for the "QCD improved" parton model

$$\nu W_2(x, Q^2) = \sum_f e_f^2 x P_f(x, Q^2), \tag{9}$$

where $P_f(x, Q^2)$ is the number density of quarks, measured to be bare at scale $\Delta x_\perp = 1/Q$, having longitudinal momentum fraction x. In terms of local operators

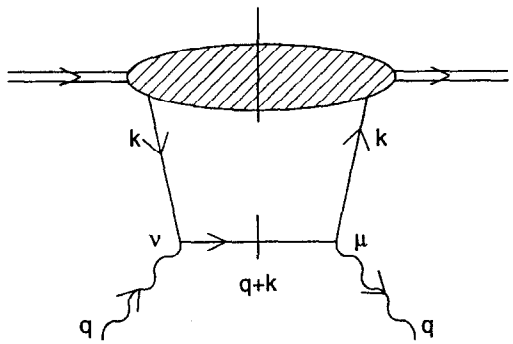

Figure 2.

$$\int_0^1 dx x^{n-1} P_f(x,Q^2) = \frac{(2\pi)^3 E_\mu}{p_+^n} (p|\tilde{q}_f \gamma_{\mu_1} i\partial_{\mu_2} \cdots i\partial_{\mu_n} q_f|p)|_{\mu_i=+}, \tag{10}$$

where the operator is renormalized at scale Q^2. In general, one should write $D_\mu = \partial_\mu - igA_\mu$ instead of ∂_μ in Eq. (10); however, in light-cone gauge $A_+ = 0$ and $D_\mu = \partial_\mu$. It is only in this gauge that the partonic picture of deep inelastic scattering is manifest.

The renormalization scale dependence, Q^2, in Eqs. (9) and(10) is governed by the DGLAP equation and is expressed most simply in terms of flavor singlet, flavor nonsinglet, and gluon distributions

$$\Delta_{ff'} = q_f(x,Q^2) - q_{f'}(x,Q^2) \tag{11a}$$

$$\Sigma = \Sigma_f \left(q_f(x,Q^2) + q\bar{f}(x,Q^2) \right) \tag{11b}$$

$$G(x,Q^2) \tag{11c}$$

as

$$Q^2 \frac{\partial}{\partial Q^2} \Delta(x,Q^2) = \frac{\alpha(Q^2)}{2\pi} \int_x^1 \frac{dx'}{x'} \gamma_{qq}(x/x') \Delta(x',Q^2) \tag{12a}$$

and

$$Q^2 \frac{\partial}{\partial Q^2} \begin{pmatrix} \Sigma(x,Q^2) \\ G(x,Q^2) \end{pmatrix} = \frac{\alpha(Q^2)}{2\pi} \int_x^1 \frac{dx'}{x'} \begin{pmatrix} \gamma_{qq}(x/x') & \gamma_{qG}(x/x') \\ \gamma_{Gq}(x/x') & \gamma_{GG}(x/x') \end{pmatrix} \cdot \begin{pmatrix} \Sigma(x',Q^2) \\ G(x',Q^2) \end{pmatrix}. \tag{12b}$$

3 Small-x Behavior from the DGLAP Equation

3.1 Leading Double Logarithms

For very small values of x, the gluon distribution and γ_{GG} dominate DGLAP evolution. The physical reason for this is clear. Soft gluons can be emitted from harder quarks or gluons, while in a gluon splitting into a quark-antiquark pair, the quark and antiquark share the momentum of the gluon equally. In the leading double-logarithm approximation, one requires a logarithm from transverse momentum integration along with a logarithm from longitudinal momenta for each power of α. In this approximation, gluons are not allowed to split into quark-antiquark pairs but only to break into an asymmetric pair consisting of a hard gluon and a soft gluon. Thus

$$Q^2 \frac{\partial}{\partial Q^2} G(x,Q^2) = \frac{\alpha(Q^2)}{2\pi} \int_x^1 \frac{dx'}{x'} \gamma_{GG}(x/x') G(x',Q^2) \tag{13}$$

is the DGLAP equation in the leading double-logarithmic approximation. Using

$$\alpha(Q^2) = \frac{1}{b\ \ell n\ Q^2/\Lambda^2}, \quad b = \frac{11N_c - 2N_f}{12\pi} \tag{14a}$$

$$\gamma_{GG}(x) = \frac{2N_c}{x} \tag{14b}$$

and writing $\ell n\ Q^2/\Lambda^2\ Q^2 \frac{\partial}{\partial Q^2} = \frac{\partial}{\partial \ell n\ \ell n\ Q^2/\Lambda^2}$, one finds

$$\frac{\partial}{\partial \ell n\ 1/x} \frac{\partial}{\partial \ell n\ \ell n\ Q^2/\Lambda^2} xG(x,Q^2) = \frac{N_c}{\pi b}\ xG(x,Q^2). \tag{15}$$

Equation (15) leads to a small-x dependence

$$xG(x,Q^2) \propto exp\left\{2\sqrt{\frac{N_c}{\pi b}\,\ell n\ 1/x \ell n(\frac{\ell n Q^2/\Lambda^2}{\ell n\ Q_0^2/\Lambda^2})}\right\}. \tag{16}$$

If one parametrizes $xG(x,Q^2)$ as a constant times $x^{-\lambda(x,Q^2)}$ in a local region of x and Q^2, then Eq. (16) leads to

$$\lambda(x,Q^2) = \sqrt{\frac{N_c}{\pi b}\,\frac{\ell n(\frac{\ell n Q^2/\Lambda^2}{\ell n Q_0^2/\Lambda^2})}{\ell n\ 1/x}}. \tag{17}$$

Since $\sqrt{\frac{N_c}{\pi b}} = \frac{6}{5}$ for $N_f = 3$, λ need not be small so long as x is not too small and so long as Q_0^2/Λ^2 is not too large. Thus, DGLAP evolution can give a fairly steep rise of $xG(x,Q^2)$, and hence of $P_f(x,Q^2)$, as x becomes small.

3.2 Deep Inelastic Scattering from DGLAP in General

The DGLAP equations furnish a general formalism for describing deep inelastic scattering in QCD. From the operator product expansion (factorization)

$$\nu W_2(x,Q^2) = \sum_{i=f,G}\int_x^1 \frac{dx'}{x'} P_i(x',Q^2) E_i(x/x',\alpha(Q^2)), \tag{18}$$

with E_i the coefficient function and P_i the parton distribution. E_i is expressed as a power series in $\alpha(Q^2)$ with the first term being $e_i^2\delta(x/x'-1)$ and leading to Eq. (9). Although the separation between P and E in Eq. (18) is in the renormalization scheme department, as one goes beyond Eq. (9), the product is scheme independent up to powers in $1/Q^2$. The parton distributions satisfy the DGLAP equation

$$Q^2\frac{\partial}{\partial Q^2} P_i(x,Q^2) = \sum_j \int_x^1 \frac{dx'}{x'}\gamma_{ij}(x/x',\alpha(Q^2)) P_j(x',Q^2). \tag{19}$$

The anomalous dimension matrix has a perturbative expansion

$$\gamma(z,\alpha) = \alpha\gamma^{(1)}(z) + \alpha^2\gamma^{(2)}(z) + \cdots. \tag{20}$$

The level of approximation in solving Eq. (19) and in describing νW_2 in terms of Eq. (18) is as follows: (i) If one keeps only $\gamma^{(1)}$ in Eq. (20) and sets $E_i = e_i^2$, one has a first-order formalism, the leading logarithmic approximation. (ii) The second-order formalism keeps the α and α^2 terms in γ along with the constant and order α terms in E_i. This is the current level of precision of the QCD description of hard processes [7-9], though in the near future, we may expect to see the third-order formalism come into use.

So long as $\alpha\ \ell n\ 1/x$ is small, the second-order QCD formalism is quite accurate. However, $\gamma^{(n)}(x)$ has terms of size $(\ell n\ 1/x)^n$ so that one can no longer expect a second-order formalism to be adequate when $\alpha\ \ell n\ 1/x$ is of order one or greater. In this case, one might expect that one should try to resum all terms of size $(\alpha \ell n 1/x)^n$ in γ and also in E_i. This resummation can be done, at the leading $\ell n\ 1/x$ level [10-16], using the BFKL equation which we shall describe later.

3.3 Physical Picture of DGLAP Evolution

DGLAP evolution describes how parton distributions change as one measures the partons with better and better resolution in $x_\perp = 1/Q$. For example, a quark which looks bare at a scale Q_0 may actually be found to be a quark and a gluon when measured with a resolution $Q > Q_0$. The situation is pictured in Fig. 3. Although DGLAP evolution can lead to large parton distributions at small x and at large Q^2, a fixed-order DGLAP formalism, when consistently used, always leads to partons being dilute in the proton. Thus the DGLAP equation, even at small x, does not lead to any new domain of QCD. As we shall see later, BFKL

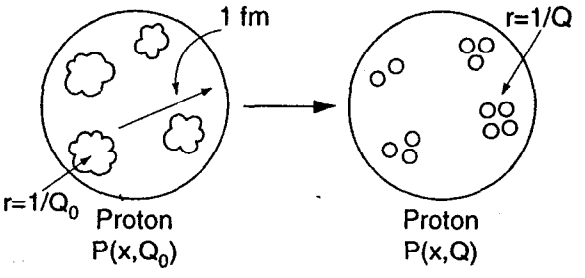

Figure 3.

evolution leads to large numbers of partons which become dense, and strongly overlap, leading to a new domain of QCD where partons can no longer be viewed as dilute and noninteracting.

4 DGLAP as BFKL

DGLAP evolution applies to two-scale problems where (at least) one of the scales is hard. For example, in deep inelastic lepton-proton scattering, the size of the proton, 1 fm, furnishes one scale while Q^2 furnishes the second, hard scale. DGLAP evolution, in a fixed-order formalism, furnishes the information on the hard-scale dependence in terms of initial conditions giving the parton distributions at a scale Q_0^2. The situation is illustrated in Fig. 4. In moving from lower Q^2 to higher Q^2 values, $\ell n\ 1/x$ always increases, as seen in Eq. (19). So long as the final x-value is not too small, the slope in Fig. 4 will not be large and a fixed-order formalism is quite adequate.

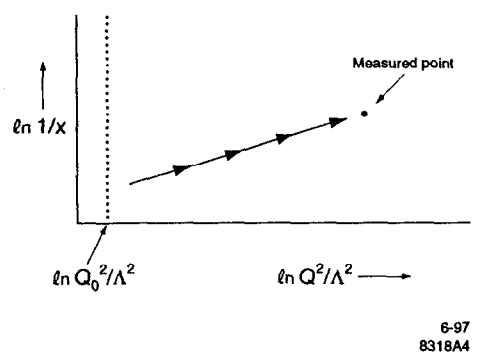

Figure 4.

If the final x-value is very small, DGLAP evolution may follow different types of paths as shown in Fig. 5. For path 1, the slope of the evolution is not large and a fixed-order DGLAP evolution should be adequate. However, for a path like 2, the AB part of that path should be well-described by low-order DGLAP evolution; however, the BC part of that path has a large slope and cannot be expected to be reliably described by fixed-order DGLAP. It is in such a circumstance where one must resum all $(\alpha \ell n\ 1/x)^n$ terms in the anomalous dimension when using Eq. (19) and do a corresponding resummation for the coefficient function in Eq. (18).

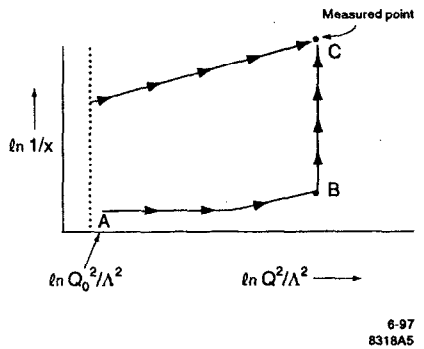

Figure 5.

While one use of the BFKL equation is to aid in the resummation of $(\alpha \ell n 1/x)^n$ terms in the anomalous dimensions and coefficient functions in a DGLAP description of deeply inelastic scattering, the BFKL equation applies directly to certain physical processes. The characteristics that a scattering process must have in order that BFKL evolution apply are: (i) there should be only one transverse momentum scale, Q, in the process; (ii) that scale should be hard enough that $\alpha(Q^2) << 1$; (iii) the center-of-mass energy squared, s, should be large enough so that $s/Q^2 >> 1$. In these circumstances, all $(\alpha \ell n\ s/Q^2)^n$ terms will be given by the BFKL equation, and thus predictions for the energy dependence will emerge. Such processes are not easy to find in practice. We shall describe several possibilities later on. *Conceptually*, the most straightforward process is heavy onium-heavy onium scattering at high energy. The only transverse scale is the size of the onium which, if the onium is heavy enough, will be in the domain of weak coupling. We shall use onium-onium scattering in the next section, as a means of describing the physics of the BFKL equation.

5 The BFKL Equation

As mentioned above, we shall use heavy onium-heavy onium scattering [17-18] as a means to describe BFKL evolution. Later on, we shall discuss specific ways that one might test BFKL evolution in more phenomenologically practical situations.

5.1 Lowest Order

Consider, in the center-of-mass system, the scattering of a heavy onium having momentum P on a heavy onium having momentum P'. We begin by treating the heavy onium state as simply a heavy quark-heavy antiquark state bound by Coulomb interactions. Then the square of the light-cone wavefunction for the state P can be described in terms of the transverse coordinates $\underline{x}_0$ and $\underline{x}_1$ of the heavy quark and heavy antiquark, respectively, along with $1-z_1$ and z_1 giving the (respective) longitudinal momentum fractions of the heavy quark and the heavy antiquark. Since the ground state wavefunction can only depend on $x_{01} = |\underline{x}_1 - \underline{x}_0|$, we may write $\Phi = \Phi(x_{01}, z_1)$ for the square of the wavefunction. Then, at lowest order, the cross section is given by the square of the one gluon exchange amplitude, shown in Fig. 6, and takes the form

$$\sigma = \int d^2x_{01} \int_0^1 dz_1 \Phi(x_{01}, z_1) \int d^2x'_{01} \int_0^1 dz'_1 \Phi(x'_{01}, z'_1) \sigma_{dipole} \tag{21}$$

with

$$\sigma_{dipole} = 2\pi\alpha^2 x_<^2 (1 + \ell n\ (x_>/x_<)) \tag{22}$$

the cross section for scattering a color dipole of size x_{01} on a color dipole of size x'_{01} at high energy. In Eq. (22), $x_< = min\{x_{01}, x'_{01}\}$ and $x_> = max\{x_{01}, x'_{01}\}$. The cross section in Eq. (21) is clearly proportional to $\alpha^2 R^2$ with R the radius of the onium.

In Coulomb gauge, the energy dependence of high-energy onium-onium scattering comes from the higher Fock space states of the onia, consisting of a heavy quark, a heavy antiquark, and some number of (virtual) transverse gluons. At the leading logarithmic level, one need only consider a single gluon exchange between the two onia in order to calculate the total onium-onium cross section.

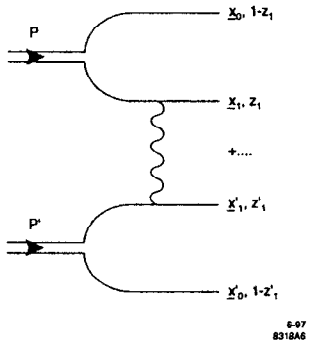

Figure 6.

5.2 One Soft Gluon in the Wavefunction in the Large-N_c Limit

In the leading logarithmic approximation, the gluons in the onium wavefunction carry a small fraction of the onium's momentum. Thus, in the one-gluon approximation, the gluon can be viewed as coming off either the heavy quark or heavy antiquark external leg as illustrated in the left-hand part of Fig. 7. In the large N_c limit, the gluon may be viewed as a quark-antiquark pair, as far as color factors are concerned. And since further soft gluon emission will only involve classical (eikonal) vertices, the gluon, in fact, acts exactly as a quark-antiquark pair at a definite transverse coordinate position. This is emphasized in the right-hand part of Fig. 7.

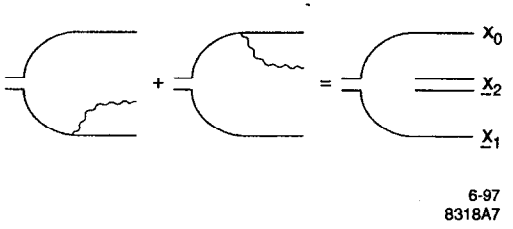

Figure 7.

5.3 Scattering in the Leading Logarithmic Approximation

In the large N_c limit, the n-gluon component of the onium wavefunction may be viewed as $n+1$ dipoles made of the (color connected) heavy quark-heavy antiquark and n "quark-antiquark pairs" corresponding to the n gluons. In an onium-onium scattering, one dipole in the right-moving onium interacts with one dipole in the left-moving onium with a cross section given by Eq. (22). Thus, we may express the total onium-onium cross section as

$$\sigma(Y) = \int \frac{d^2x d^2x'}{4\pi^2 x^2 x'^2} N(x, Y/2) N(x', Y/2) \sigma_{dipole}(x, x'), \tag{23}$$

where $N(x, Y/2)$ is number density of dipoles of transverse size $x = |\underline{x}|$ formed using gluons in a rapidity interval $Y/2$, where $Y = \ell n(s/M^2)$ with $s = p \cdot p'$ and with M the onium mass. Thus, in order to calculate the high-energy cross section, we need to know the dipole density in an onium state.

5.4 The BFKL Equation

In order to write an equation for N, it is convenient to first write

$$N(x, Y) = \int d^2x_{01} \int_0^1 dz_1 \Phi(x_{01}, z_1) n(x_{01}, x, Y), \tag{24}$$

where $n(x_{01}, x, Y)$ has the simple interpretation of the number density of dipoles of size x in a rapidity interval Y starting with a (parent) dipole of size x_{01}. The creation of dipoles proceeds by one gluon emission which changes a single dipole into two dipoles as illustrated in Fig. 7.

The equation for n is given as

$$n(x_{01}, x, Y) = x\delta(x - x_{01}) exp\{-\frac{2\alpha N_c}{\pi} \ell n(\frac{x_{01}}{\rho}) Y\} +$$

$$+ \frac{\alpha N_c}{\pi^2} \int_R \frac{x_{01}^2 d^2x_2}{x_{02}^2 x_{21}^2} \int_0^Y dy \; exp\{\frac{-2\alpha N_c}{\pi} \ell n \, (\frac{x_{01}}{\rho})(Y - y)\} n(x_{21}, x, y), \tag{25}$$

and is illustrated in Fig. 8. The gluon $(\underline{x}_2, y)$ is the hardest of the soft gluons in the wavefunction of the onium. The subscript R on the integral in Eq. (25) indicates that one is to integrate over the region $x_{02}, x_{21} \geq \rho$. The introduction of ρ serves to cut off ultraviolet divergences in the wavefunction. ρ appears correspondingly in the virtual corrections [the exponential factors in Eq. (25)] which are determined from probability conservation. As always in a BFKL description, only leading logarithms [terms of the type $(\alpha Y)^n$] are kept in Eq. (25), although transverse coordinate expressions are exact, up to powers of ρ which will be unimportant when the $\rho \to 0$ limit is taken for a physical quantity.

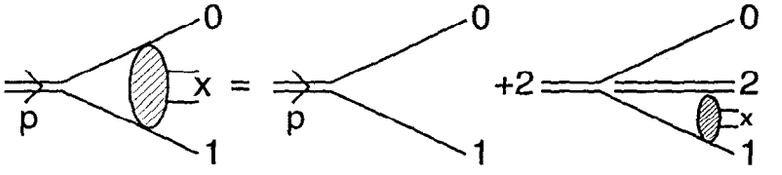

6-97
8318A8

Figure 8.

Taking a derivative with respect to Y on both sides of Eq. (25) gives

$$\frac{dn(x_{01}, x, Y)}{dY} = \frac{\alpha N_c}{\pi^2} \int_R d^2x_2 \{\frac{x_{01}^2}{x_{02}^2 x_{12}^2} - 2\pi\delta(\underline{x}_2 - \underline{x}_0) \ell n \frac{x_{01}}{\rho}\} n(x_{21}, x, Y). \tag{26}$$

The limit $\rho \to 0$ can be taken after performing the integration in Eq. (26). Equation (26) is the BFKL equation expressing the evolution of the number of gluons (dipoles) as one changes the available longitudinal momentum region which those gluons are allowed to occupy.

5.5 The Solution to the BFKL Equation

The solution to Eq. (26) is

$$n(x_{01}, x, Y) = \frac{x_{01}}{2x} \frac{e^{(\alpha_P - 1)Y}}{\sqrt{\frac{7}{2}\alpha \, N_c \zeta(3) Y}} \, exp\{\frac{-\pi \ell n^2(x_{01}/x)}{14\alpha \, N_c \zeta(3) Y}\} \tag{27}$$

with $\alpha_P - 1 = \frac{4\alpha N_c}{\pi}\ell n 2$. Using Eq. (27) in Eq. (23) and Eq. (24) gives

$$\sigma = \frac{16\pi R^2 \alpha^2 e^{(\alpha_P - 1)Y}}{\sqrt{\frac{7}{2}\alpha N_c \zeta(3) Y}} \tag{28}$$

with

$$R = 1/2 \int d^2 x_{01} \int_0^1 dz_1 x_{01} \Phi(x_{01} z_1) \tag{29}$$

the onium radius.

From Eq. (28), we see that σ becomes larger than the geometric cross section πR^2 when $Y \approx \frac{1}{\alpha_P - 1}\ell n\ 1/\alpha^2$ so it is at such rapidities that one expects strong (unitarity) corrections to the BFKL equation to become important.

5.6 The Physical Picture of BFKL Evolution

Earlier, we saw that DGLAP evolution corresponds to a growing number of gluons in a state as one looks to smaller and smaller transverse distances, and that this growth is especially strong when a large longitudinal phase space is available. In BFKL evolution, the focus is on evolution for a fixed transverse size as one increases the available longitudinal phase space. The picture is illustrated in Fig. 9 with the formula given in Eq. (27). Equation (27) shows that in addition to a growth in Y of the number of dipoles (gluons), there is also a diffusion of dipoles sizes away from the starting size, x_{01} in Eq. (27). In principle, this diffusion is slow enough, compared to the rate of growth of the number of gluons, that the picture of the growth of the number of gluons of a fixed size as shown in Fig. 9, a hot spot of gluons in the proton, is a reasonably good picture of BFKL evolution. However, there are circumstances where the diffusion inherent in BFKL evolution is very important and cannot be neglected [19].

5.7 Unitarity, Saturation, and High Field Strengths

With proper triggering on final-state characteristics, one should be able to discuss questions of unitarity, saturation, and high field strengths in the context of two hot spots colliding in a proton-proton collision. However, we prefer to keep the discussion simple and conceptual, so again, high-energy onium-onium scattering

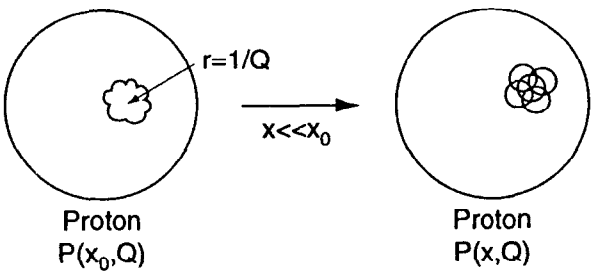

Figure 9.

will be our "theoretical laboratory" for these topics. In the center of mass, we may express, crudely, onium-onium scattering as

$$\sigma \approx [N(Y/2)]^2 \sigma_{dipole}, \tag{30}$$

where we have simplified Eq. (23) by taking a typical dipole size in the integral appearing there. Again, crudely, $\sigma_{dipole} \approx \alpha^2 R^2$ so that σ is of size R^2, where unitarity corrections can be expected to become important, when Y is large enough so that $N(Y/2) \approx 1/\alpha$. As we have seen earlier, this corresponds to $Y \approx \frac{1}{\alpha_P - 1}\ell n\ 1/\alpha^2$. Thus, we expect the BFKL approximation to break down when the center-of-mass wavefunctions have on the order of $1/\alpha$ dipoles (gluons) spread over a rapidity interval $Y/2$. The number of dipoles (gluons) per unit rapidity, $\frac{dN(Y/2)}{d(Y/2)}$, is a constant when $N \approx 1/\alpha$ so that the field strength, $F_{\mu\nu}$, in the wavefunction is of order one for those gluons occupying the lowest unit of rapidity. (The field strengths coming from gluons in any other unit of rapidity in the wavefunction are even smaller.) Since $F_{\mu\nu}$ is not large, we expect unitarity corrections to be calculable perturbatively, and this is indeed the case. Including the dominant unitarity corrections in high-energy onium-onium scattering can be done, and numerical calculations are available [17,20,21]. Unitarity corrections in the center-of-mass system are just the multiple scattering corrections involving two or more dipoles.

Perturbation theory is expected to break down when $F_{\mu\nu}$ takes on values as large as $1/g$ for gluons occupying a unit of rapidity. This occurs, in the center-of-

mass frame, when $\frac{dN(Y/2)}{d(Y/2)} \approx 1/\alpha$ which corresponds to rapidity $Y = \frac{2}{\alpha_P - 1} \ell n\ 1/\alpha^2$, a rapidity twice that necessary for unitarity corrections to become important. At rapidities this large, the number of gluons in the wavefunctions becomes so large that our whole perturbative picture of the wavefunction breaks down and a new nonperturbative regime of QCD is reached. Unfortunately, one cannot expect to reach such a regime at Fermilab or HERA energies.

6 Phenomenology

6.1 The Soft Pomeron

There are clearly strong similarities between small-x physics and high-energy soft hadronic processes. Unfortunately, high-energy soft processes are very difficult to deal with in QCD. For example, $\sigma = \sigma_0(s/s_0)^\epsilon$, with $\epsilon \approx 0.08$, gives a good fit to many cross sections [22,23], including total photoabsorption as measured up through HERA energies. ϵ is a nonperturbative parameter which should be calculable in QCD. However, in the present Euclidean formulations of lattice QCD, one cannot give an algorithm for calculating ϵ, and in fact, it is likely that it is not possible to calculate ϵ in an Euclidean formulation of lattice QCD. So for the moment, it is difficult to make progress in soft hadronic physics, and we await a successful formulation of nonperturbative QCD where such extremely Minkowskian quantities, such as ϵ, can be calculated. A good candidate for such a formulation is discrete light-cone QCD.

6.2 $\nu W_2(x, Q^2)$, Quark and Gluon Distributions

For $Q^2 \geq 1.5\ GeV^2$, νW_2 rises rapidly with decreasing x with the rate of rise depending somewhat on the exact value of Q^2 (Ref. [24]). For $Q^2 \leq 0.6\ GeV^2$, νW_2 acts like a soft process with a moderate, $x^{-\epsilon}$, x-dependence which appears independent of Q^2. It will be interesting to have data in the $0.6 < Q^2 < 1.5$ region to see exactly how the transition from hard to soft physics comes about. Also, very precise data in the $1\ GeV^2 \leq Q^2 \leq 5\ GeV^2$ regime could give evidence for, or against, the necessity of resummation effects in a DGLAP description of deep inelastic scattering. This is clearly a phenomenology of pressing urgency at the moment.

On a more qualitative level, in the region $10\ GeV^2 \leq Q^2 \leq 20\ GeV^2$ and $x \approx 10^{-4}$, the number of quarks and antiquarks per unit of rapidity in the proton is about four while the number of gluons is likely between 20 and 30. These are rather extraordinary numbers when one recalls that a traditional gluon distribution $G(x) = \frac{3}{x}(1-x)^5$ used for intermediate values of x corresponds to three gluons per unit rapidity. It would be very interesting to have gluon densities in the lower Q^2 regime. It might be that gluon densities become large enough for saturation efffects [25] to become important in the $Q^2 \approx 1\ GeV^2$ regime.

6.3 Rapidity Gaps Bounded by Jets

We now turn to some specific processes of special interest in small-x physics. The first of these, rapidity gaps bounded by jets, may furnish a window to BFKL behavior. Such events have now been studied both at Fermilab [26,27] and at HERA [28]. In each case, one measures two jets having $k_\perp \geq Q$ with a rapidity gap between them. Except for the measured jets and the rapidity gap, the process is otherwise inclusive [29-31]. One might guess that such a cross section would take the form

$$\sigma_{2jet}^{gap} = x_1 q_1(x_1, Q^2) \hat{\sigma}(Y, Q^2) x_2 q_2(x_2, Q^2) \tag{31}$$

with x_1 and x_2 being the momentum fractions of the two jets and q_1 and q_2 being the quark and/or antiquark distributions from which the jets emerge. (For simplicity of discussion, we ignore gluons.) The process is illustrated in Fig. 10. Furthermore, one might suppose that

$$\hat{\sigma} \propto \frac{e^{2(\alpha_P - 1)Y}}{Y^3}, \tag{32}$$

thus furnishing a possibility of measuring the BFKL Pomeron.

However, the process is not inclusive enough to use the hard scattering formula (31). The problem is that requiring a rapidity gap destroys the delicate cancellation between real and virtual soft gluons, of which cancellation is key to a factorization such as expressed in Eq. (31). One knows how to write the cross section for the hard elastic quark-quark scattering $\hat{\sigma}$, but the probability that there are no accompanying soft interactions between the spectator quarks, which would fill in the gap, is not something which can be calculated perturbatively. What has

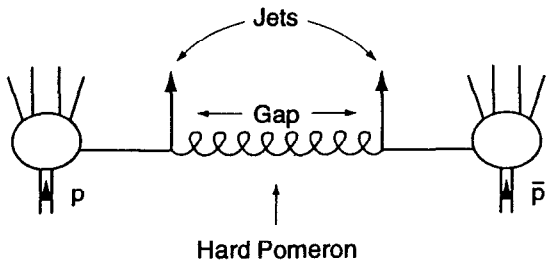

Fig. 10.

become traditional is to include a factor [32,33] $< S^2 >$ on the right-hand side of Eq. (31), interpreted as the survial probability of the gap, or equivalently, the probability of no soft spectator interactions.

Data from Fermilab show that about 1% of two-jet events have a gap of greater that two to three units of rapidity while at HERA that number is about 5%. This means that $< S^2 > \approx 0.1$ at Fermilab and $< S^2 > \approx 0.5$ at HERA. If $< S^2 >$ is not very energy dependent and this is likely, one can take ratios of gap events at $E = 1800\ GeV$ to those at $E = 630\ GeV$ now that Fermilab has data at two energies. Keeping x_1 and x_2 the same at the two energies, Eq. (31) leads to

$$\frac{\sigma^{gap}_{2-jet}(1800\ GeV)}{\sigma^{gap}_{2-jet}(630\ GeV)} = e^{4(\alpha_P-1)\ell n\ 3}\left[\frac{Y(630)}{Y(1800)}\right]^3 \frac{< S^2 >_{1800}}{< S^2 >_{630}}. \tag{33}$$

For example, if $Y(630) = 4$ then $Y(1800) \approx 6$ and

$$\frac{\sigma(1800)}{\sigma(630)} \approx \frac{8}{27}\frac{< S^2 >_{1800}}{< S^2 >_{630}} \cdot e^{4(\alpha_P-1)}, \tag{34}$$

or assuming that $< S^2 >$ does not increase with energy,

$$\frac{\sigma(1800)}{\sigma(630)} \leq \frac{8}{27}\, e^{4(\alpha_P-1)}. \tag{35}$$

If $\alpha_P - 1 = 1/2$, this ratio could be as large as 2. It will be interesting to see what happens when the data is analyzed.

6.4 Diffractive Vector Meson Production [34-37]

The process $\gamma(Q) + proton \to V + proton'$ with V a vector meson is illustrated in Fig. 11. We suppose that Q^2 is large, although for heavy vector mesons, this need not be the case in order to carry out an analysis similar to the one outlined here.

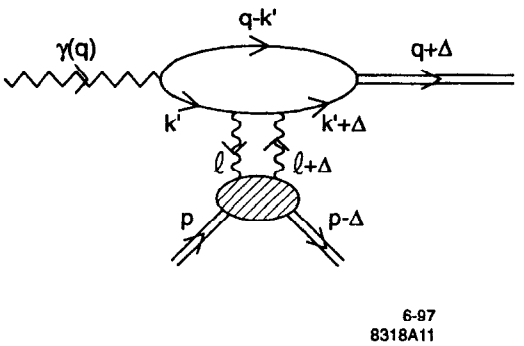

Fig. 11.

The amplitude is expected to be dominated by two-gluon exchange to the $\gamma - V$ system. We suppose that $t = \Delta^2$ is very small. In the rest system of the target proton, the process proceeds in three steps.

(i) Before reaching the target, $\gamma(Q)$ goes, virtually, into a quark-antiquark pair having lifetime

$$\tau_i = \frac{2qz(1-z)}{Q^2 z(1-z) + k_\perp^2 + m^2} \approx \frac{2q}{Q^2}, \tag{36}$$

where z is the fraction of the photon's momentum carried by the antiquark, $k_z = zq_z$. For example, for $Q^2 = 5\ GeV^2$ and $q = 100\ GeV, \tau_i = 8\ fm$.

(ii) The quark-antiquark pair scatters off the target. Since the $k_\perp^2$ integration is only cut off at Q^2, the quark-antiquark pair has $\Delta x_\perp \sim 1/Q$, meaning that the coupling of the gluons, lines ℓ and $\ell + \Delta$, occur with $\alpha(Q^2)$ strength. This justifies perturbation theory. In coupling to the small dipole moment of the quark-antiquark pair, one gets a factor of $\ell_\perp^2$ from lines ℓ and $\ell + \Delta$. This factor of $\ell_\perp^2$ gives a logarithmic $\ell_\perp^2-$ integral, again cut off at Q^2. The $\ell_\perp^2$-integral is exactly the same as appears in defining the gluon distribution.

(iii) The vector meson is formed from the quark-antiquark pair at a time

$$\tau_f = \frac{2qz(1-z)}{k_\perp^2 + m^2}, \tag{37}$$

with m the quark mass. One finds, for longitudinally polarized virtual photons,

$$\left.\frac{d\sigma_{\gamma^*+N\to V+N'}}{dt}\right|_{t=0} = \frac{12\pi^3}{\alpha_{em}Q^6N_c^2}\Gamma_{V\to e^+e^-}m_V\alpha^2(Q^2)\eta_V^2|xG(x,Q^2)+i\frac{\pi}{c}\frac{d}{dx}xG|^2 \tag{38}$$

with

$$x = \frac{Q^2+m_V^2}{s} \tag{39}$$

and

$$\eta_V = \frac{1}{2}\frac{\int_0^1 \frac{dz}{z(1-z)}\Phi_V(z)}{\int_0^1 dz\Phi_V(z)} \tag{40}$$

given in terms of the exclusive wavefunction Φ_V of the vector meson.

Equation (38) has been derived in a double-leading logarithmic approximation. Further refinements, necessary to confront data, can be found in Ref. 36. At the moment, perhaps the main use of Eq. (41) is to get an independent check on the gluon distribution which occurs quadratically in the diffractive cross section. Data at HERA [24] have already found the extremely rapid rise of the diffractive cross section with decreasing x expected from a gluon distribution now known to grow rapidly at small x.

6.5 The Search for the BFKL Pomeron

6.5.1 Deep Inelastic Scattering

Precise studies of νW_2 may give evidence for resummation effects [13-16]. This would be an indirect confirmation of BFKL dynamics, but one cannot directly measure $\alpha_P - 1$ from νW_2 data alone. Final state properties, such as transverse energy flow, may also prove useful in deciding how important BFKL dynamics is in deep inelastic scattering, but so far these analyses have not proved very definitive.

6.5.2 Gaps at Fermilab and HERA

I think the best hope here is a comparison of gaps bounded by jets in the two Fermilab energies as given by Eq. (33). The difficulty is that the Y^{-3} prefactors to BFKL behavior suppress the 1800 GeV to 630 GeV ratio so that this measurement will only prove successful if $\alpha_P - 1$ is near $1/2$ and if the survival probability is not very energy dependent. However, a ratio of two or more in the gap cross section comparing 1800 GeV data to 630 GeV data would be a definitive sign of BFKL dynamics, and one could try to extract $\alpha_P - 1$, or at least bounds on that quantity.

6.5.3 Large-t Vector Meson Diffractive Photoproduction [38]

Earlier, we have seen that t=0 diffractive electroproduction of vector mesons gives a measurement of the gluon distribution of the proton, at least in the leading double logarithmic approximation. If one takes $-t$ large, say $-t \geq 3\ GeV^2$ or so, the diffractive cross section has the asymptotic form

$$\frac{d\sigma}{dt} \propto \frac{(s/(-t))^{2(\alpha_P-1)}}{(\ell n\ (s/(-t))^3)} \tag{41}$$

and could furnish a determination of $\alpha_P - 1$. The most favorable measurement is to allow the proton to break up so that a quark jet takes the recoil transverse momentum of the vector meson. In some respects, this process is like the gap events bounded by jets which were discussed earlier, now with one of the jets replaced by a vector meson. There is no survival probability factor because the incoming photon is pointlike and has no spectators to interact with the target proton. However, the cross sections here are small, and apparently, the asymptotic behavior sets in rather slowly. Nevertheless, it will be interesting to see what emerges from the HERA data.

6.5.4 Associated Jets in Proton-Antiproton and Electron-Proton Collisions

One straightforward way to measure the BFKL intercept, $\alpha_P - 1$, is to study the inclusive two-jet cross section at Fermilab [39,40] or the associated one-jet cross section at HERA [41-43]. Let me illustrate the idea in terms of the Fermilab process. In a proton-antiproton collision, one measures two jets, inclusively, having

momentum fractions x_1 and x_2 and transverse momenta $k_{1\perp}, k_{2\perp} \geq Q$ with Q a fixed (perturbative) scale. The process is illustrated in Fig. 12.

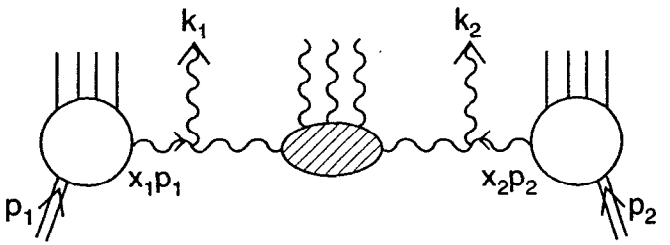

Figure 12.

The two-jet cross section is

$$\sigma_{2-jet} = x_1[G(x_1,Q^2) + \frac{4}{9}(q+\bar{q})(x_1,Q^2)]x_2[G(x_2,Q^2) + \frac{4}{9}(q+\bar{q})(x_2,Q^2)]$$

$$\cdot \left(\frac{\alpha N_c}{\pi}\right)^2 \frac{\pi^3}{2Q^2} \frac{e^{(\alpha_P - 1)Y}}{\sqrt{\frac{7}{2}\alpha N_c \zeta(3) Y}}, \tag{42}$$

where Y is the relative rapidity of the two measured jets. If one takes the ratio of σ_{2-jet}, keeping x_1, x_2, and Q^2 fixed, at 1800 GeV and 630 GeV, the result is

$$\frac{\sigma_{2-jet}(1800)}{\sigma_{2-jet}(630)} = e^{2(\alpha_P - 1)\ell n 3} \sqrt{\frac{Y(630)}{Y(1800)}} \tag{43}$$

so long as $Y(630)$ is large enough to use the asymptotic form (42). For example, for $Y(630) = 4$, one gets $Y(1800) = 6$, and the ratio in Eq. (43) is about 2 for $(\alpha_P - 1) = 1/2$. While Eq. (42) is only a leading logarithmic formula, a significant growth in the two-jet cross section with energy would be a significant beginning to a BFKL phenomenology. There should be a Fermilab result on this soon.

The corresponding measurement at HERA, a forward inclusive jet measurement, has been vigorously pursued by the H1 Collaboration [44]. The preliminary results are strongly encouraging and seem to agree reasonably with the BFKL prediction [44,45]. More definitive comparisons between theory and experiment can be expected soon and are eagerly awaited.

7 What Is Needed

From the experimental side, the most urgent issue is a measurement of the BFKL Pomeron, that is, a measurement of $\alpha_P - 1$. Also, extremely precise data in the low-x and low to intermediate Q^2-region for νW_2 will be very useful. We can expect the level of phenomenology to improve to the point of deciding how well second order DGLAP fits really work and to what level resummation effects are important. Also, a good direct measurement of $xG(x,Q^2)$ either from two forward jet production or from heavy quark production is important to test how well second order DGLAP evolution works and to have confidence in the values of xG.

From the theory side, the α^2 correction to $\alpha_P - 1$ is very important in order to do BFKL phenomenology with a good level of confidence. We desperately need a better understanding of the $Q^2 \approx 1$ regime, where perturbative and nonperturbative physics merge. Finally, from a purely theory point of view, clarification and a deeper understanding of unitarity corrections, saturation effects and their relationship to high field strength QCD are exciting areas where further progress should be possible.

References

[1] Y. L. Dokshitzer, Sov. Phys. JETP **73**, 1216 (1977).

[2] V. N. Gribov and L. N. Lipatov, Sov. J. Nucl. Phys. **15**, 78 (1972).

[3] G. Altarelli and G. Parisi, Nucl. Phys. B **126**, 298 (1977).

[4] E. A. Kuraev, L. N. Lipatov, and V. S. Fadin, Sov. Phys. JETP **45**, 199 (1978).

[5] Y. Y. Balitsky and L. N. Lipatov, Sov. J. Nucl. Phys. **28**, 22 (1978).

[6] L. N. Lipatov, "Small-x physics in perturbative QCD," hep-ph/9610276 (1996).

[7] A. D. Martin, R. G. Roberts, and W. J. Stirling, Phys. Rev. D **50**, 6734 (1994); Phys. Lett B **387**, 419 (1996).

[8] CTEQ Collaboration: J. Botts *et al.*, Phys. Lett. B **304**, 159 (1993); H. L. Lai *et al.*, Phys. Rev. D **51**, 4763 (1995); Phys. Rev. D **55**, 1280 (1997).

[9] M. Glück, E. Reya, and A. Vogt, Z. Phys. C **67**, 433 (1995).

[10] T. Jaroszewicz, Phys. Lett. B **116**, 291 (1982).

[11] S. Catani, M. Ciafaloni, and F. Hautmann, Nucl. Phys. B **366**, 135 (1991).

[12] S. Catani and F. Hautmann, Nucl. Phys. B **427**, 475 (1994).

[13] R. K. Ellis, F. Hautmann, and B. R. Webber, Phys. Lett. B **348**, 582 (1995).

[14] R. D. Ball and S. Forte, Phys. Lett. B **351**, 313 (1995); Phys. Lett. B **351**, 365 (1995).

[15] J. R. Forshaw, R. G. Roberts, and R. S. Thorne, Phys. Lett. B **356**, 79 (1995).

[16] R. S. Thorne, Phys. Lett. B **392**, 463 (1997).

[17] A. H. Mueller, Nucl. Phys. B **415**, 373 (1994); Nucl. Phys. B **437**, 107 (1995).

[18] A. H. Mueller and B. Patel, Nucl. Phys. B **425**, 471 (1994).

[19] J. Bartels and H. Lotter, Phys. Lett. B **309**, 400 (1993).

[20] G. Salam, Nucl. Phys. B **461**, 512 (1996).

[21] A. H. Mueller and G. Salam, Nucl. Phys. B **475**, 293 (1996).

[22] K. Goulianos, Phys. Reports **101**, 169 (1983).

[23] A. Donnachie and P. V. Landshoff, Nucl. Phys. B **244**, 322 (1984); B **267**, 690 (1985).

[24] See, for example, the lectures of W. Smith at this school.

[25] L. V. Gribov, E. M. Levin, and M. G. Ryskin, Phys. Reports **100**, 1 (1983).

[26] DØ Collaboration, S. Abachi *et al.*, Phys. Rev. Lett. **72**, 2332 (1994).

[27] CDF Collaboration, F. Abe *et al.*, Phys. Rev. Lett. **74**, 855 (1995).

[28] ZEUS Collaboration, M. Derrick *et al.*, Phys. Lett. B **369**, 55 (1996).

[29] J. D. Bjorken, Int. J. Mod. Phys. A **7**, 4189 (1992).

[30] A. H. Mueller and W.-K. Tang, Phys. Lett. B **284**, 123 (1992).

[31] V. Del Duca and W.-K. Tang, Phys. Lett. B **312**, 225 (1993).

[32] J. D. Bjorken, Phys. Rev. D **47**, 101 (1992).

[33] E. Gotsman, E. M. Levin, and U. Maor, Phys. Lett. B **309**, 199 (1993).

[34] M. G. Ryskin, Z. Phys. C **57**, 89 (1993).

[35] S. J. Brodsky, L. Frankfurt, J. F. Gunion, A. H. Mueller, and M. Strikman, Phys. Rev. D **50**, 3134 (1994).

[36] L. Frankfurt, W. Koepf, and M. Strikman, Phys. Rev. D **54**, 3194 (1996).

[37] A. D. Martin, M. G. Ryskin, and T. Teubner, Phys. Rev. D **55**, 4329 (1997).

[38] J. R. Forshaw and M. Ryskin, Z. Phys. C **68**, 137 (1995).

[39] A. H. Mueller and H. Navelet, Nucl. Phys. B **282**, 727 (1987).

[40] V. Del Duca and C. R. Schmidt, Phys. Rev. D **49**, 4510 (1994); D **51**, 2150 (1995).

[41] W.-K. Tang, Phys. Lett. B **278**, 363 (1992).

[42] J. Bartels, A. DeRoeck, and M. Loewe, Z. Phys. C **54**, 635 (1992).

[43] J. Kwiecinski, A. Martin, and P. J. Sutton, Phys. Rev. D **461**, 921 (1992).

[44] H1 Collaboration, paper pa 03-049 submitted to the *28th International Conference on High Energy Physics*, Warsaw, Poland, July 1996.

[45] J. Bartels *et al.*, Phys. Lett B **384**, 300 (1996).